Pergamon

Int. J. Heat Mass Transfer. Vol. 41, Nos 6–7, pp. 825–837, 1998

Printed in Great Britain
0017-9310/98 $19.00+0.00

PII: S0017-9310(97)00183-X

Influence of liquid bridge volume on instability of floating half zone convection

Q. S. CHEN and W. R. HU
Institute of Mechanics, CAS, Bejing 100080, People's Republic of China

(*Received* 23 *June* 1997)

Abstract—Thermocapillary instabilities on floating half zone convection in microgravity environment were investigated by linear instability analysis method. The critical Marangoni numbers were obtained and compared with the experimental ones. The influences of the liquid bridge volume and the aspect ratio on the critical Marangoni number were analyzed. It is found that the liquid bridge volume and the aspect ratio have great influence on the critical Marangoni number. There was a gap region where the oscillatory convection will not be observed in present analyses and in experiments in the curve of the critical Marangoni number vs the liquid bridge volume for the case of large Prandtl number and small aspect ratio. © 1997 Elsevier Science Ltd.

1. INTRODUCTION

Thermocapillary flow is of importance in many applications such as crystal growth, and the instability mechanism of the thermocapillary flow is also needed to be explored. The temperature fluctuation mechanism in thermocapillary flow is sensitive for the industry applications. Although thermocapillary instability of liquid layer with free surface has been proposed by Pearson [1] in 1958, several other instability mechanisms considering the capillary flow have also been proposed by others [2–6]. The convective instability mechanism of liquid layer has been proposed by Smith [2, 3]. Since the basic flow and the temperature distribution in their analyses are chosen linear distribution, and the endwalls' effects have not been considered using parallel flow approximation. The effects of the endwalls of liquid bridge on the critical Marangoni number will be discussed later. For experimental cases, the temperature distribution in the center part of liquid bridge of large aspect ratio may be considered as linear distribution, but the temperature distribution near the wall is not uniform especially for liquid bridge of small aspect ratio, the mechanism proposed may account for the temperature fluctuation mechanism for the liquid bridge with large aspect ratio. The same mechanism of convection instability is also supported by Kuhlmann [4, 5]. In their analyses, the endwalls' effects have been considered, but the effects of the volume size have not been considered. Other oscillatory mechanism associated with buoyancy force has been proposed by Hu [6]. Nearly all analyses focus on a liquid bridge of cylinder, which is a special case. General configuration of liquid bridge deviates from the cylinder, and it is expected that the liquid bridge volume is another important critical parameter and has obviously influence on the critical Marangoni number. This influence was studied by experiment [7] and direct numerical simulation [8] for medium of 10 cst silicon oil. Present paper will study the oscillatory convection by the linear instability analysis method, and the results may cover a relative larger parameter range. The Prandtl number of transparent medium limits in $Pr \in [1, 10^2]$, and this range of Prandtl number will be analyzed in the present paper. The second section will be mathematical description, the third section is results and discussions and the last is conclusion.

2. LINEAR INSTABILITY ANALYSIS

The usual half zone model which has constant temperatures on both rods has often been used to investigate the role of thermocapillary convection in floating zone crystal growth processes [9]. The schematic model of the usual floating half zone is shown in Fig. 1, the liquid with free surface is bounded between the two rods. A cylindrical coordinate system is used and the origin of coordinates is located at the middle of the lower rod. The flow field and temperature distribution in a liquid bridge are considered in the Boussinesq approximation. Zero gravity is assumed in the present paper. The non-dimensional parameters of the system are listed below:

$$Pr = \frac{\nu}{\alpha}, \quad Re = \frac{U_0 R_0}{\nu},$$

$$Ma = Re \cdot Pr = \frac{|\sigma_T'| \Delta T R_0}{\rho \nu \alpha}, \quad Bi = \frac{hR_0}{k}, \quad A = \frac{L}{2R_0} \tag{1}$$

where Pr, Re, Ma, Bi, A denote Prandtl, Reynolds, Marangoni and Biot number and aspect ratio of the liquid bridge, respectively. L is the gap between the

NOMENCLATURE

A	aspect ratio, $L/2R_0$
Bi	Biot number, hR_0/k
h	thermal transfer coefficient [J m^{-2} s^{-1} K^{-1}]
J	integer denoting the last grid station in a radial direction
k	thermal conductivity of liquid [J m^{-1} s^{-1} K^{-1}]
L	the gap between the two rods [m]
m	azimuthal wave number
Ma	Marangoni number, $\lvert\sigma_T'\rvert\Delta TR_0/\rho\nu\alpha$
N	integer denoting the last grid station in an axial direction
p	dimensionless perturbed pressure
Pr	Prandtl number, ν/α
p_0	dimensionless basic pressure
r	dimensionless radial coordinate
R	dimensionless radius of the free surface
R'	differentiation of R with respect to z, dR/dz
Re	Reynolds number, U_0R_0/ν
R_0	radius of the rod [m]
t	dimensionless time
T	dimensionless perturbed temperature
T_j	the jth degree Chebyshev polynomial
T_n	the nth degree Chebyshev polynomial
T_L	temperature on the lower rod [K]
T_0	dimensionless basic temperature
ΔT	temperature difference between the upper rod and the lower rod [K]
u	dimensionless perturbed radial velocity
u_0	dimensionless basic radial velocity
U_0	reference velocity, $\lvert\sigma_T'\rvert\Delta T/\rho\nu$
v	dimensionless perturbed azimuthal velocity
w	dimensionless perturbed axial velocity
w_0	dimensionless basic axial velocity
z	dimensionless axial coordinate.

Greek symbols

α	thermal diffusivity
δ	width of the upper and lower parts on the free surface where the stress balance condition are modified
ε	amplitude of perturbation
θ	azimuthal anger
ν	kinematic viscosity of liquid [m^2 s^{-1}]
ρ	density of liquid [kg m^{-3}]
σ	eigenvalue, $\sigma_r + i\sigma_i$
σ_i	image part of eigenvalue
σ_r	real part of eigenvalue
σ_T'	surface tension differentiation with respect to temperature [N m^{-1} K^{-1}].

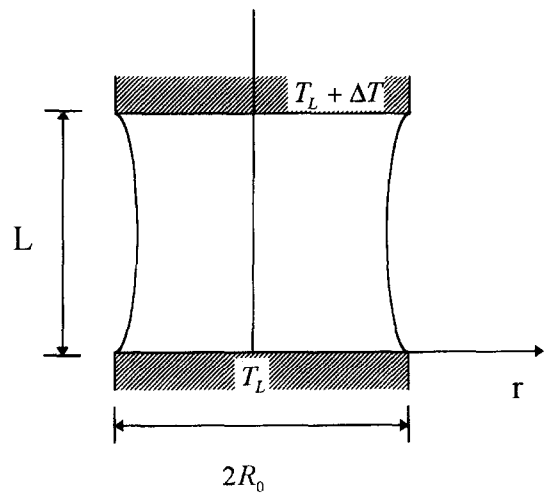

Fig. 1. Schematic drawing of the usual floating half zone heating from above.

two rods, R_0 is the radius of the rod and ΔT is the applied temperature difference between the upper and lower rods. The reference velocity $U_0 = \lvert\sigma_T'\rvert\Delta T/\rho\nu$, reference length scale is chosen as R_0 and reference time scale is R_0/U_0. Constants ρ, ν, k, α, h, σ_T' denote density, kinematic viscosity, thermal conductivity, thermal diffusivity, thermal transfer coefficient and surface tension differentiation with respect to temperature, respectively.

In linear instability analysis of thermocapillary convection in the usual floating half zone, the basic flow and temperature distribution are essential for the exact value of critical Marangoni number. The basic flow and temperature distribution have been obtained by numerical computation of axisymmetric thermocapillary convection in the usual floating half zone using spectral method [9]. The small amplitude fluctuation of the velocities $\mathbf{u} = (u, v, w)$, pressure p and temperature T are imposed to the basic state $\mathbf{u}_0 = (u_0, 0, w_0)$, p_0 and T_0 as follows:

$$\begin{pmatrix} u_0 \\ 0 \\ w_0 \\ p_0 \\ T_0 \end{pmatrix} + \varepsilon \begin{pmatrix} u \\ v \\ w \\ p \\ T \end{pmatrix} \tag{2}$$

where the perturbation parameter ε is small in order of magnitude. The small amplitude fluctuation equations may be expressed as follows:

$$\frac{\partial \mathbf{u}}{\partial t}+\mathbf{u}\cdot\nabla\mathbf{u}_0+\mathbf{u}_0\cdot\nabla\mathbf{u}=-\nabla p+\frac{1}{Re}\nabla^2\mathbf{u}$$

$$\nabla\cdot\mathbf{u}=0$$

$$\frac{\partial T}{\partial t}+\mathbf{u}\cdot\nabla T_0+\mathbf{u}_0\cdot\nabla T=\frac{1}{RePr}\nabla^2 T. \tag{3}$$

The boundary conditions at the rods ($z=0$ and $2A$) are the same ones of usual floating half zone model [9].

Equation (3) may be rewritten in the cylindrical coordinate system as follows,

$$\frac{1}{r}\frac{\partial(ru)}{\partial r}+\frac{1}{r}\frac{\partial v}{\partial\theta}+\frac{\partial w}{\partial z}=0 \tag{4a}$$

$$\frac{\partial u}{\partial t}+u_0\frac{\partial u}{\partial r}+w_0\frac{\partial u}{\partial z}+u\frac{\partial u_0}{\partial r}+w\frac{\partial u_0}{\partial z}=-\frac{\partial p}{\partial r}+\frac{1}{Re}\times\left(\frac{\partial^2 u}{\partial r^2}+\frac{1}{r}\frac{\partial u}{\partial r}-\frac{u}{r^2}+\frac{\partial^2 u}{r^2\partial\theta^2}+\frac{\partial^2 u}{\partial z^2}-2\frac{\partial v}{r^2\partial\theta}\right) \tag{4b}$$

$$\frac{\partial v}{\partial t}+u_0\frac{\partial v}{\partial r}+w_0\frac{\partial v}{\partial z}+\frac{u_0 v}{r}=-\frac{\partial p}{r\partial\theta}+\frac{1}{Re}\times\left(\frac{\partial^2 v}{\partial r^2}+\frac{1}{r}\frac{\partial v}{\partial r}-\frac{v}{r^2}+\frac{\partial^2 v}{r^2\partial\theta^2}+\frac{\partial^2 v}{\partial z^2}+\frac{2}{r^2}\frac{\partial u}{\partial\theta}\right) \tag{4c}$$

$$\frac{\partial w}{\partial t}+u_0\frac{\partial w}{\partial r}+w_0\frac{\partial w}{\partial z}+u\frac{\partial w_0}{\partial r}+w\frac{\partial w_0}{\partial z}=-\frac{\partial p}{\partial z}+\frac{1}{Re}\left(\frac{\partial^2 w}{\partial r^2}+\frac{1}{r}\frac{\partial w}{\partial r}+\frac{\partial^2 w}{r^2\partial\theta^2}+\frac{\partial^2 w}{\partial z^2}\right) \tag{4d}$$

$$\frac{\partial T}{\partial t}+u_0\frac{\partial T}{\partial r}+w_0\frac{\partial T}{\partial z}+u\frac{\partial T_0}{\partial r}+w\frac{\partial T_0}{\partial z}=\frac{1}{RePr}\left(\frac{\partial^2 T}{\partial r^2}+\frac{1}{r}\frac{\partial T}{\partial r}+\frac{\partial^2 T}{r^2\partial\theta^2}+\frac{\partial^2 T}{\partial z^2}\right). \tag{4e}$$

The small perturbation quantities (u, v, w, p, T) could be suggested in the following forms:

$$\begin{bmatrix} u\\ v\\ w\\ p\\ T\end{bmatrix}=\sum_{m=0}^{\infty} e^{\sigma t+im\theta}\begin{bmatrix}\tilde{u}_m(r,z)\\ im\tilde{v}_m(r,z)\\ \tilde{w}_m(r,z)\\ \tilde{p}_m(r,z)\\ \tilde{T}_m(r,z)\end{bmatrix}+\text{c.c.} \tag{5}$$

where $\sigma=\sigma_r+i\sigma_i$, σ_r and σ_i are, respectively, the increasing rate and frequency of small perturbation, m denotes the azimuthal wave number, i denotes the complex unit $\sqrt{-1}$, and c.c. denotes the complex conjugate. Distribution (5) gives a spectrum of perturbation, and the discussion is focused in a single mode m. In this case, the subscript m will be omitted for simplification. Applying the curl operation throughout eqns (4b)–(4d) and eliminating the pressure term, following equation may be obtained:

$$\frac{\partial\tilde{u}}{\partial r}+\frac{\tilde{u}}{r}-\frac{m^2}{r}\tilde{v}+\frac{\partial\tilde{w}}{\partial z}=0 \tag{6a}$$

$$\frac{\partial}{\partial t}\left(\tilde{u}-r\frac{\partial\tilde{v}}{\partial r}-\tilde{v}\right)+\left(u_0\frac{\partial\tilde{u}}{\partial r}+w_0\frac{\partial\tilde{u}}{\partial z}+\tilde{u}\frac{\partial u_0}{\partial r}+\tilde{w}\frac{\partial u_0}{\partial z}\right)-\frac{\partial}{\partial r}\left(ru_0\frac{\partial\tilde{v}}{\partial r}+rw_0\frac{\partial\tilde{v}}{\partial z}+u_0\tilde{v}\right)=\frac{1}{Re}\left(\frac{\partial^2\tilde{u}}{\partial r^2}+\frac{1}{r}\frac{\partial\tilde{u}}{\partial r}-\frac{1+m^2}{r^2}\tilde{u}+\frac{\partial^2\tilde{u}}{\partial z^2}+\frac{2m^2}{r^2}\tilde{v}\right)-\frac{1}{Re}\frac{\partial}{\partial r}\left[r\left(\frac{\partial^2\tilde{v}}{\partial r^2}+\frac{1}{r}\frac{\partial\tilde{v}}{\partial r}-\frac{1+m^2}{r^2}\tilde{v}+\frac{\partial^2\tilde{v}}{\partial z^2}+\frac{2}{r^2}\tilde{u}\right)\right] \tag{6b}$$

$$\frac{\partial}{\partial t}\left(\frac{\partial\tilde{v}}{\partial z}-\frac{\tilde{w}}{r}\right)+\frac{\partial}{\partial z}\left(u_0\frac{\partial\tilde{v}}{\partial r}+w_0\frac{\partial\tilde{v}}{\partial z}+\frac{u_0\tilde{v}}{r}\right)-\frac{1}{r}\left(u_0\frac{\partial\tilde{w}}{\partial r}+w_0\frac{\partial\tilde{w}}{\partial z}+\tilde{u}\frac{\partial w_0}{\partial r}+\tilde{w}\frac{\partial w_0}{\partial z}\right)=\frac{1}{Re}\frac{\partial}{\partial z}\left(\frac{\partial^2\tilde{v}}{\partial r^2}+\frac{1}{r}\frac{\partial\tilde{v}}{\partial r}-\frac{1+m^2}{r^2}\tilde{v}+\frac{\partial^2\tilde{v}}{\partial z^2}+\frac{2}{r^2}\tilde{u}\right)-\frac{1}{Re}\frac{1}{r}\left(\frac{\partial^2\tilde{w}}{\partial r^2}+\frac{1}{r}\frac{\partial\tilde{w}}{\partial r}-\frac{m^2}{r^2}\tilde{w}+\frac{\partial^2\tilde{w}}{\partial z^2}\right) \tag{6c}$$

$$\frac{\partial\tilde{T}}{\partial t}+u_0\frac{\partial\tilde{T}}{\partial r}+w_0\frac{\partial\tilde{T}}{\partial z}+\tilde{u}\frac{\partial T_0}{\partial r}+\tilde{w}\frac{\partial T_0}{\partial z}=\frac{1}{RePr}\left(\frac{\partial^2\tilde{T}}{\partial r^2}+\frac{1}{r}\frac{\partial\tilde{T}}{\partial r}-\frac{m^2}{r^2}\tilde{T}+\frac{\partial^2\tilde{T}}{\partial z^2}\right). \tag{6d}$$

The above equations must be satisfied with the following boundary conditions.

At $z=0$ and $2A$:

$$\tilde{u}=0,\quad \tilde{v}=0,\quad \tilde{w}=0,\quad \frac{\partial\tilde{w}}{\partial z}=0,\quad \tilde{T}=0. \tag{7}$$

At $r=R(z)$:

$$2\left(\frac{\partial\tilde{u}}{\partial r}-\frac{\partial\tilde{w}}{\partial z}\right)R'+\left(\frac{\partial\tilde{w}}{\partial r}+\frac{\partial\tilde{u}}{\partial z}\right)(1-R'^2)=-W(z)(1+R'^2)^{1/2}\left(\frac{\partial\tilde{T}}{\partial r}R'+\frac{\partial\tilde{T}}{\partial z}\right)$$

$$\left(\frac{\partial\tilde{v}}{\partial r}-\frac{\tilde{v}}{r}+\frac{\tilde{u}}{r}\right)-R'\left(\frac{\tilde{w}}{r}+\frac{\partial\tilde{v}}{\partial z}\right)=-W(z)(1+R'^2)^{1/2}\frac{\tilde{T}}{r}$$

$$\tilde{u}-\tilde{w}R'=0$$

$$\frac{\partial\tilde{T}}{\partial r}-\frac{\partial\tilde{T}}{\partial z}R'=-(1+R'^2)^{1/2}Bi\cdot\tilde{T} \tag{8}$$

where $W(z)$ is the regularization factor applied to the upper and lower parts on the free surface, and has the following form:

$$W(z)=\begin{cases}\left[\dfrac{1-\cos(z\pi/\delta_s)}{2}\right]^2 & z\leqslant\delta_s\\ 1, & \delta_s<z<2A-\delta_s\\ \left[\dfrac{1-\cos((2A-z)\pi/\delta_s)}{2}\right]^2 & z\geqslant 2A-\delta_s\end{cases}\tag{9}$$

where σ_s is a small positive number and is adopted as the width of the upper and lower parts of the free surface where the tangential components of the stress balance condition on the free surface are modified, $\delta_s=0.2A$. the conditions at the center axis is as follows:

at $r=0$

$$m=0:\quad \tilde{u}=0,\tilde{v}=0,\frac{\partial\tilde{w}}{\partial r}=0,\frac{\partial\tilde{T}}{\partial r}=0$$

$$m=1:\quad \frac{\partial\tilde{u}}{\partial r}=0,\tilde{u}-\tilde{v}=0,\tilde{w}=0,\tilde{T}=0$$

$$m>1:\quad \tilde{u}=0,\tilde{v}=0,\tilde{w}=0,\tilde{T}=0.\tag{10}$$

The spatial discretization is base on a spectral method using Chebyshev polynomial expansions in the axial direction and the radial direction,

$$\begin{Bmatrix}\tilde{u}(r,z)\\ \tilde{v}(r,z)\\ \tilde{w}(r,z)\\ \tilde{q}(r,z)\\ \tilde{T}(r,z)\end{Bmatrix}=\sum_{j=0}^{J}\sum_{n=0}^{N}\begin{Bmatrix}\hat{u}(j,n)\\ \hat{v}(j,n)\\ \hat{w}(j,n)\\ \hat{q}(j,n)\\ \hat{T}(j,n)\end{Bmatrix}\times T_j\left[1-\frac{2r}{R(z)}\right]T_n\left(1-\frac{z}{A}\right),$$

$$(0\leqslant r\leqslant R(z),0\leqslant z\leqslant 2A)\tag{11}$$

where J, N are the orders of Chebyshev polynomial expansions in radial and longitudinal directions, respectively, T_j, T_n are the jth and nth degree Chebyshev polynomials, $\tilde{u}$, $\tilde{v}$, $\tilde{w}$, $\tilde{p}$, $\tilde{T}$ are the spectral coefficients of the corresponding velocities, pressure and temperature. The collocation grids are chosen as following:

$$(r_i,z_l)=\left[\frac{R(z)}{2}\left(1-\cos\frac{\pi i}{J}\right),\quad A\left(1-\cos\frac{\pi l}{N}\right)\right]$$

$$0\leqslant i\leqslant J,\quad 0\leqslant l\leqslant N.\tag{12}$$

The algebraic equations are obtained by substituting the variables in the equations and boundary conditions with associated Chebyshev polynomial expansions (11) at each node.

$$\sum_{j=0}^{J}\sum_{n=0}^{N}[A(r_i,z_l,j,n)-\sigma C(r_i,z_l,j,n)]\hat{\varphi}(j,n)=0,$$

$$0\leqslant i\leqslant J,\quad 0\leqslant l\leqslant N\tag{13}$$

where $\varphi(j,n)=(\hat{u},\hat{v},\hat{w},\hat{T})^{\mathrm{T}}(j,n)$, superscript T denotes transposition, A and C are square matrices. The eigenvalue and eigenfunction are obtained by the Q–R method.

3. RESULTS

The usual half zone of liquid bridge which has constant temperatures on both rods is considered in the present linear instability analyses. The basic flow pattern and temperature distribution which have axisymmetric forms were obtained by numerical calculation similar to the one in [9]. Figure 2(a–c) are the basic flow pattern in the vertical cross-section of the usual half zone of liquid bridge with $Pr=10$, $Ma=8000$, $A=0.6$ and $V=0.8$, 1 and 1.2, respectively. Figure 3(a–c) are the basic temperature distribution in the vertical cross-section of the usual half zone of liquid bridge with $Pr=10$, $Ma=8000$, $A=0.6$ and $V=0.8$, 1.0 and 1.2, respectively.

3.1. *Thermocapillary instability of the half zone of liquid bridge*

The critical Marangoni numbers for the onset of oscillatory convection with azimuthal wave number $m=0$, 1 and 2 are shown in Fig. 4 for $Pr=50$ as function of the aspect ratio. The critical curve corresponding to $m=1$ is the most unstable mode.

The perturbed flow pattern and temperature distribution are then obtained by using the linear instability method mentioned above. The perturbed temperature distribution in the vertical cross-section $\theta=0$ for the most unstable mode $m=1$ are shown in Fig. 5(a–c) for $Ma=8000$, $Pr=10$, $A=0.6$, and $V=0.8$, 1.0 and 1.2, respectively. There are a minimum temperature center in the vertical cross-section $\theta=0$ of the half zone and a maximum temperature center in the opposite vertical cross-section $\theta=\pi$. The perturbed temperature distributions for different liquid bridge volumes show different features. The perturbed flow pattern in vertical cross-section $\theta=\pi/2$ for the most unstable mode $m=1$ are shown in Fig. 6(a–c) for $Ma=8000$, $Pr=10$, $A=0.6$, and $V=0.8$, 1.0 and 1.2, respectively. From the perturbed flow pattern, it can be observed that the convection in the vertical cross-section is driven by the perturbed gradient of surface tension.

The perturbed temperature distribution in the horizontal cross-section for the most unstable mode $m=1$ are shown in Fig 7(a–c) for $Ma=8000$, $Pr=10$, $A=0.6$ and $V=0.8$, 1.0 and 1.2, respectively. The maximum and minimum temperature are distributed asymmetrically in the bulk region of the half zone of liquid bridge. The flow pattern in the horizontal cross-section for the most unstable mode $m=1$ are shown in Fig. 8(a–c) for $Ma=8000$, $Pr=10$, $A=0.6$ and $V=0.8$, 1.0 and 1.2, respectively. Two vortices are formed in the horizontal cross-section, and are also driven by the surface tension gradient in the periphery direction. The similar flow patterns in the horizontal

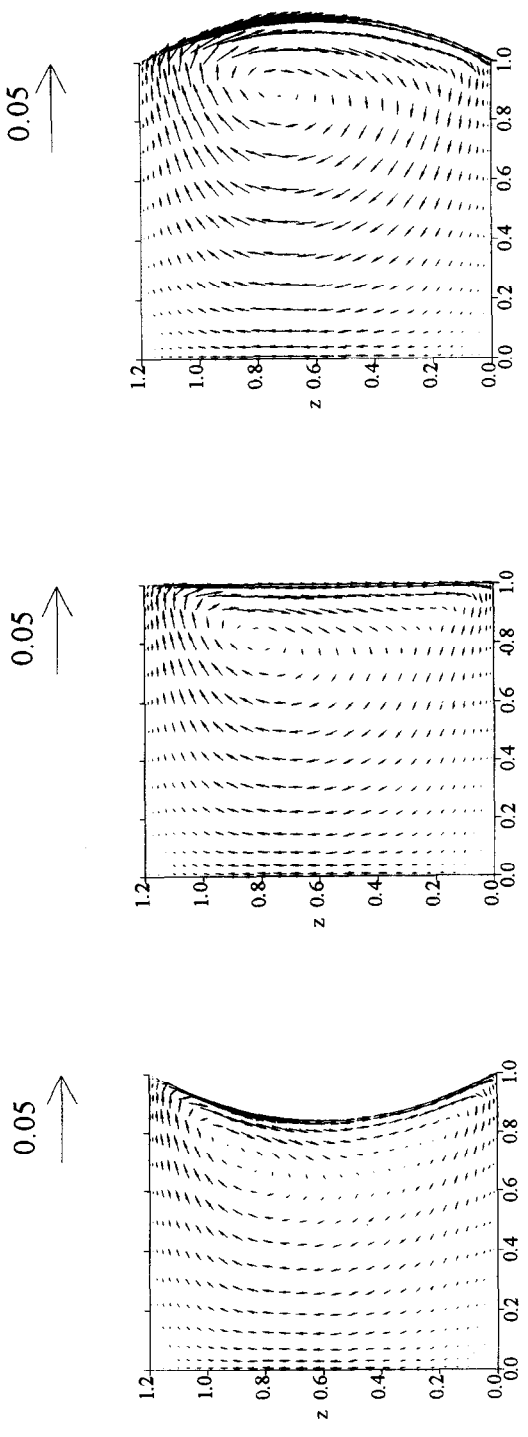

Fig. 2. The basic velocity field in the vertical cross-section of the usual floating half zone with $Pr = 10$, $Ma = 8000$, $A = 0.6$ and (a) $V = 0.8$, (b) $V = 1$, and (c) $V = 1.2$.

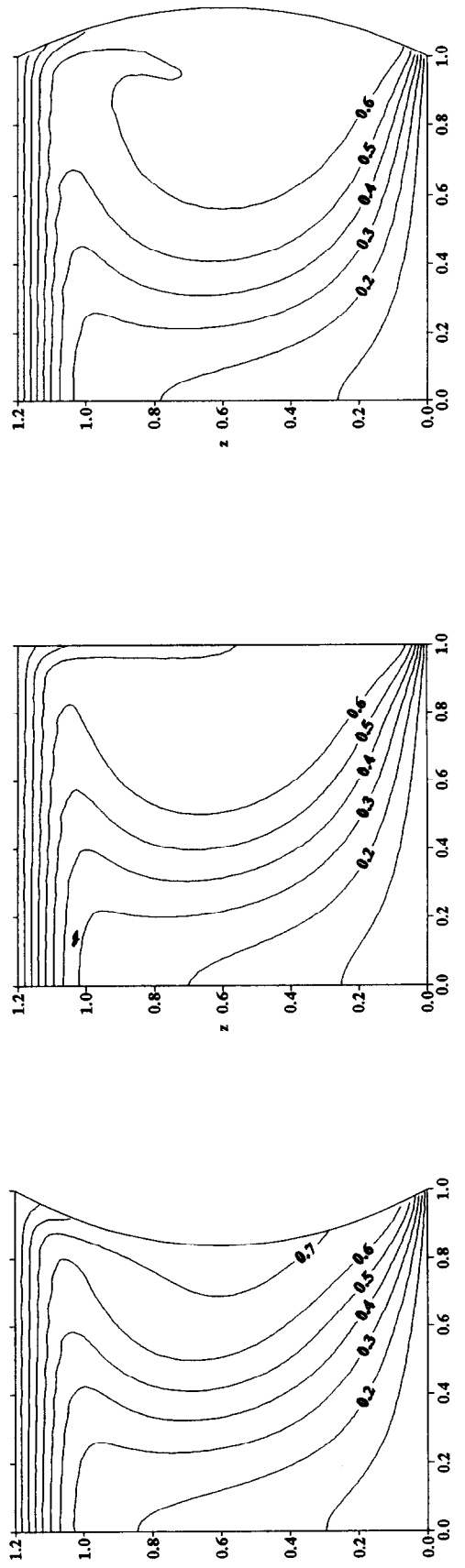

Fig. 3. The basic temperature distribution in the vertical cross-section of the usual floating half zone with $Pr = 10$, $Ma = 8000$, $A = 0.6$ and (a) $V = 0.8$, (b) $V = 1$, and (c) $V = 1.2$.

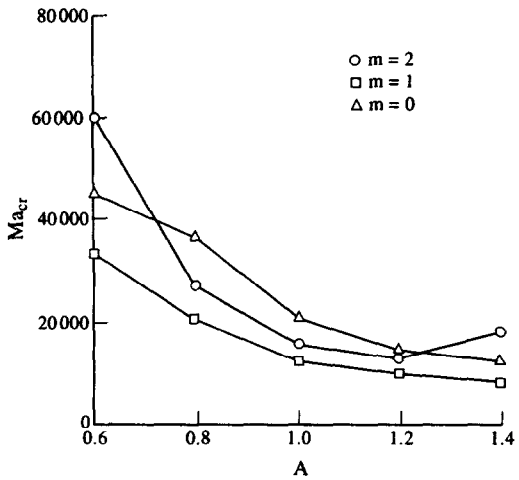

Fig. 4. Neutral curves for $V = 0.8$ and $m = 0$, 1 and 2.

cross-section were also observed in present experiments. The mechanism of temperature oscillation for large Prandtl number is initiated by the temperature oscillation on the free surface, and the asymmetric flow in the bulk region of the half zone of liquid bridge are generated by the perturbed tangential surface tension gradient which is associated with the perturbed temperature distribution on the free surface.

3.2. *Dependence of critical Marangoni number on the aspect ratio*

The dependence of the critical Marangoni number on the aspect ratio of the half zone of liquid bridge is investigated. The critical Marangoni numbers vs aspect ratio for the most unstable mode $m = 1$ are plotted for $V = 0.8$, 1.0 and 1.2 in Fig. 9(a–c) for $Pr = 1$, 10 and 50, respectively. The theoretical results of $V = 1$ can be compared with the experimental results of [10] and other numerical results [4, 5]. It can be seen the critical Marangoni number will increase when the aspect ratio decreases for constant liquid bridge volume. The critical Marangoni number will approaches a small value when the aspect ratio of liquid bridge is large enough. The critical Marangoni number of liquid bridge with small aspect ratio is larger than that of the liquid bridge with large aspect ratio.

The critical frequencies $\sigma_{r_{cr}} \cdot Re_{cr}$ for the most unstable mode $m = 1$ vs the aspect ratio are plotted for $V = 0.8$, 1 and 1.2 in Fig. 10(a–c) for Prandtl number $Pr = 1$, 10 and 50, respectively. The critical frequencies are also increased with decreasing aspect ratio, for high frequency is usually associated with higher Reynolds number.

3.3. *Dependence of critical Marangoni number on the liquid bridge volume*

The influences of the liquid bridge volume on the critical Marangoni number are also investigated. The curves of the critical Marangoni number for the most unstable mode $m = 1$ vs the liquid bridge volume for $A = 0.6$ are plotted in Fig. 11(a, b) for $Pr = 10$ and 50, respectively. The critical curves of the Marangoni number vs the liquid bridge volume obtained in this paper are compared with that in [7, 8] which discuss the case of larger Prandtl number of $Pr = 105$. In the present paper of the case $Pr = 50$ and $A = 0.6$, there exists a gap region where the oscillatory convection will not be observed in experiments [7, 8]. The critical curves consist of two branches which are corresponding to the fat bridge and slender bridge for larger Prandtl number. This conclusion agrees with the one in [7, 8]. In the case of $Pr = 10$ and $A = 0.6$, the critical curves are continue and two branches are disappeared. However, there exists regions of liquid bridge volume with relatively large critical Marangoni number, the liquid bridge volume has great influence on the critical Marangoni number.

The critical frequency $\sigma_{r_{cr}} \cdot Re_{cr}$ for the most unstable mode $m = 1$ vs the volume size of liquid bridge for $A = 0.6$ are plotted in Fig. 12(a, b) for $Pr = 10$ and 50, respectively.

4. CONCLUSION

The linear instability of axisymmetric thermocapillary flow in usual floating half zone which has constant temperatures on both rods has been investigated. The critical curves of the Marangoni number depending on the liquid bridge volume and the aspect ratio in microgravity environment have been obtained. The calculation methods including the computation of axisymmetric basic flow and the three-dimensional linear instability analyses used in the present paper are proved successful.

The mechanism of oscillatory thermocapillary convection is investigated by using linear instability method. From the calculation it can be observed that the oscillatory convection in the liquid bridge of floating half zone is driven by the gradient of the surface tension coupled with the internal process of convection. The results show the oscillatory temperature is coupled with the oscillatory flow and the oscillatory convection is generated by fluctuation of surface tension associated with the fluctuation of surface temperature for the case of large Prandtl number. The calculation results of instability analyses agree qualitatively with the experimental results and other theoretical results.

The influences of the aspect ratio on the critical Marangoni are investigated. The critical Marangoni number and the critical frequency will decrease when increasing aspect ratio and approach a limited value with rather larger aspect ratio.

The influence of the liquid bridge volume on the critical Marangoni number are also discussed. For the case of large Prandtl number and small aspect ratio, there exists a gap region where the oscillatory convection will not be observed in present analyses and experiments, two branches of the curves of the critical

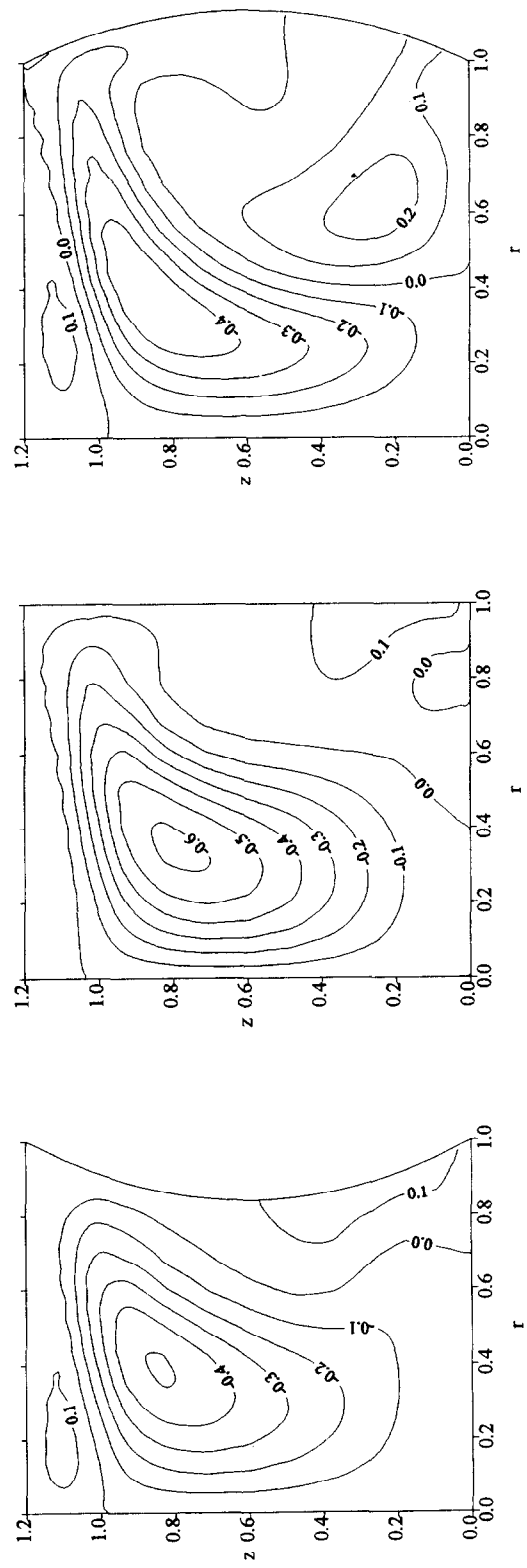

Fig. 5. The perturbed temperature distribution for the most unstable mode $m = 1$ in the vertical cross-section of the usual floating half zone with $Pr = 10$, $Ma = 8000$, $A = 0.6$ and (a) $V = 0.8$, (b) $V = 1$, and (c) $V = 1.2$.

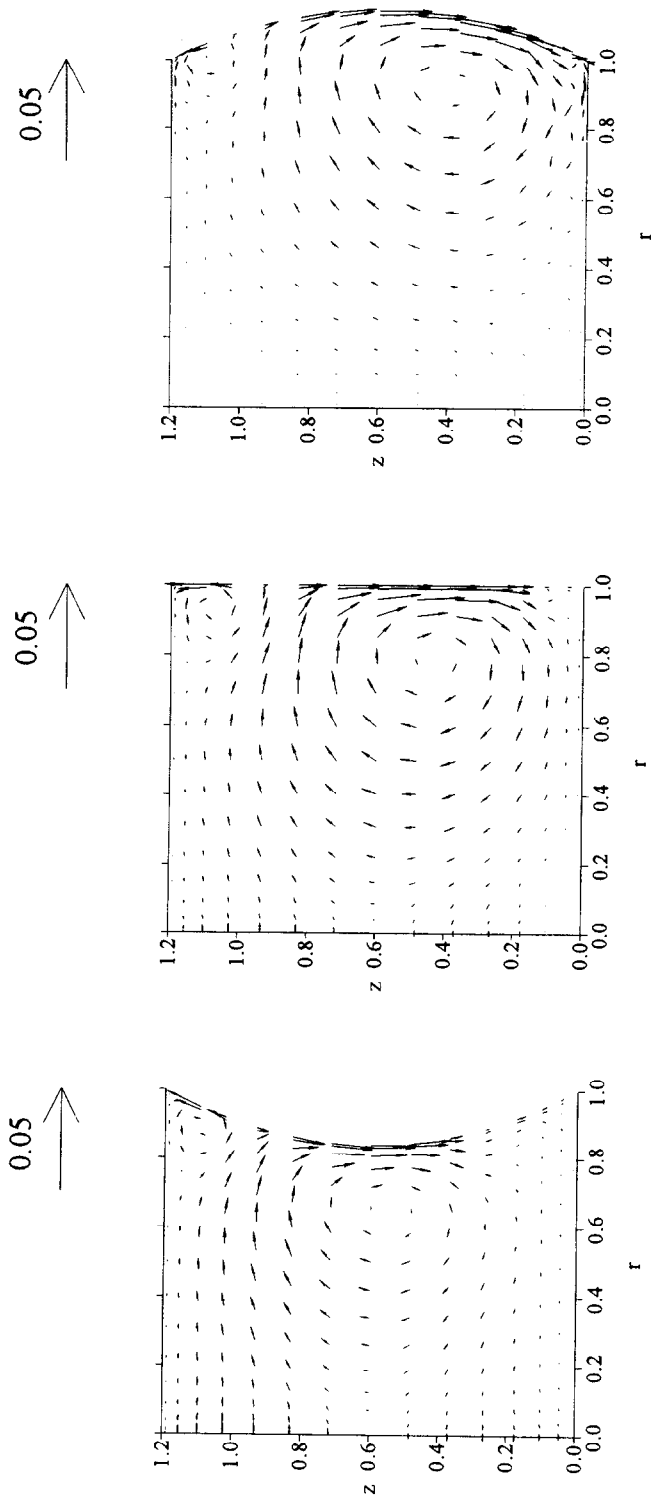

Fig. 6. The perturbed flow field for the most unstable mode $m = 1$ in the vertical cross-section of the usual floating half zone with $Pr = 10$, $Ma = 8000$, $A = 0.6$ and (a) $V = 0.8$, (b) $V = 1$, and (c) $V = 1.2$.

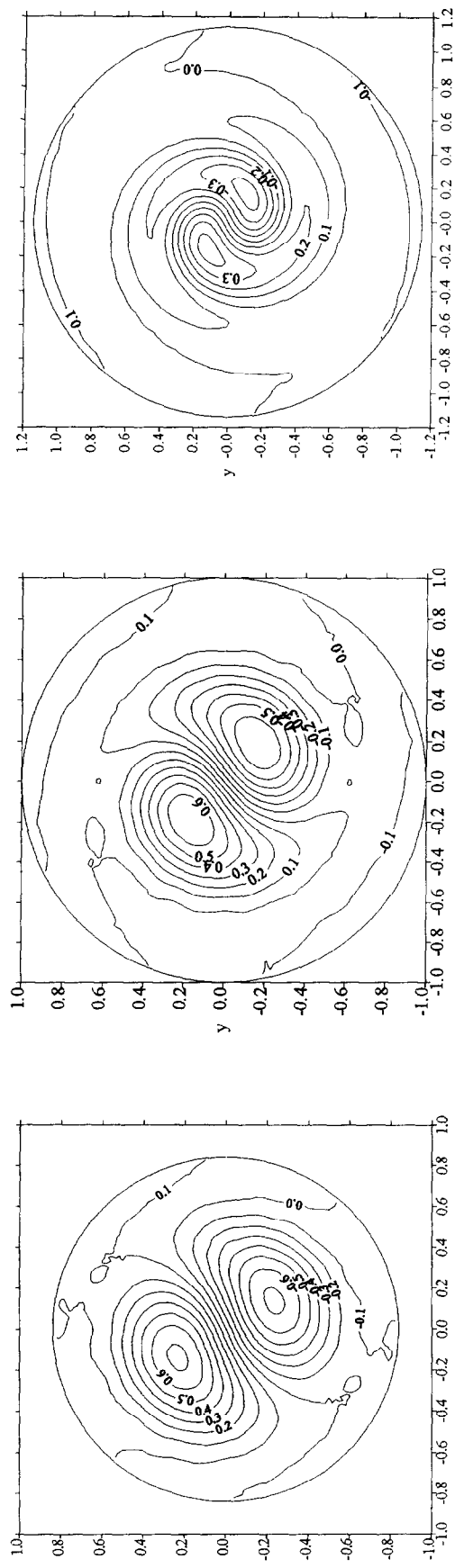

Fig. 7. The perturbed flow field for the most unstable mode $m = 1$ in horizontal cross-section of the usual floating half zone with $Pr = 10$, $Ma = 8000$, $A = 0.6$ and (a) $V = 0.8$, (b) $V = 1$, and (c) $V = 1.2$.

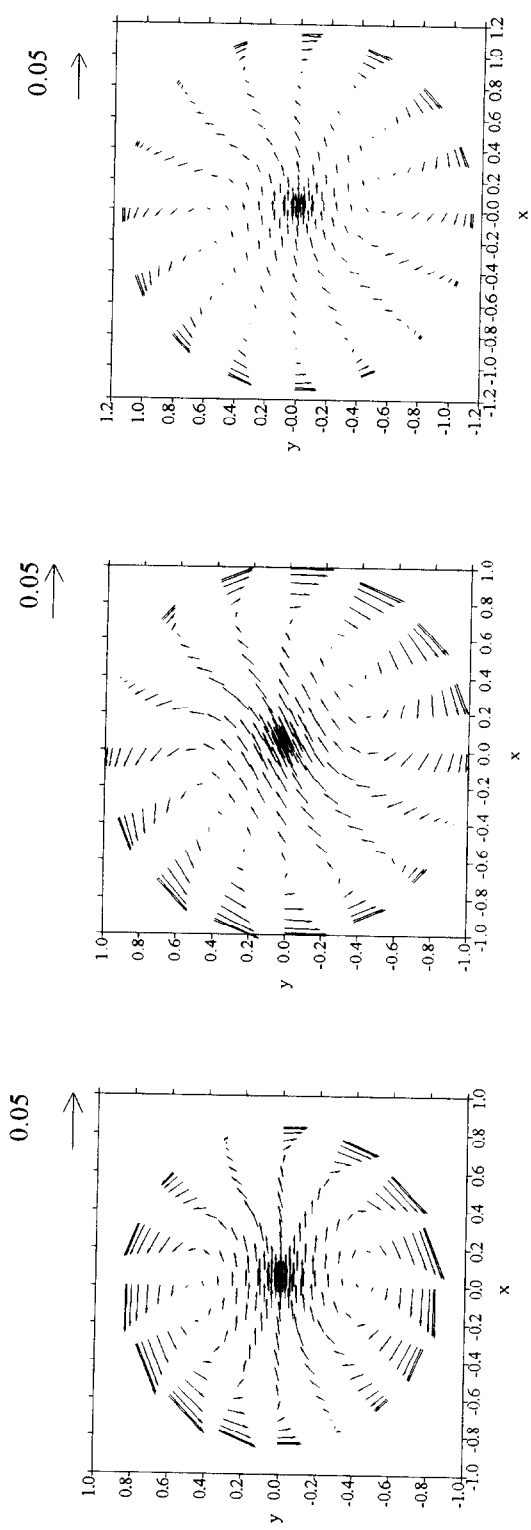

Fig. 8. The perturbed flow field for the most unstable mode $m = 1$ in horizontal cross-section of the usual floating half zone with $Pr = 10$, $Ma = 8000$, $A = 0.6$ and (a) $V = 0.8$, (b) $V = 1$, and (c) $V = 1.2$.

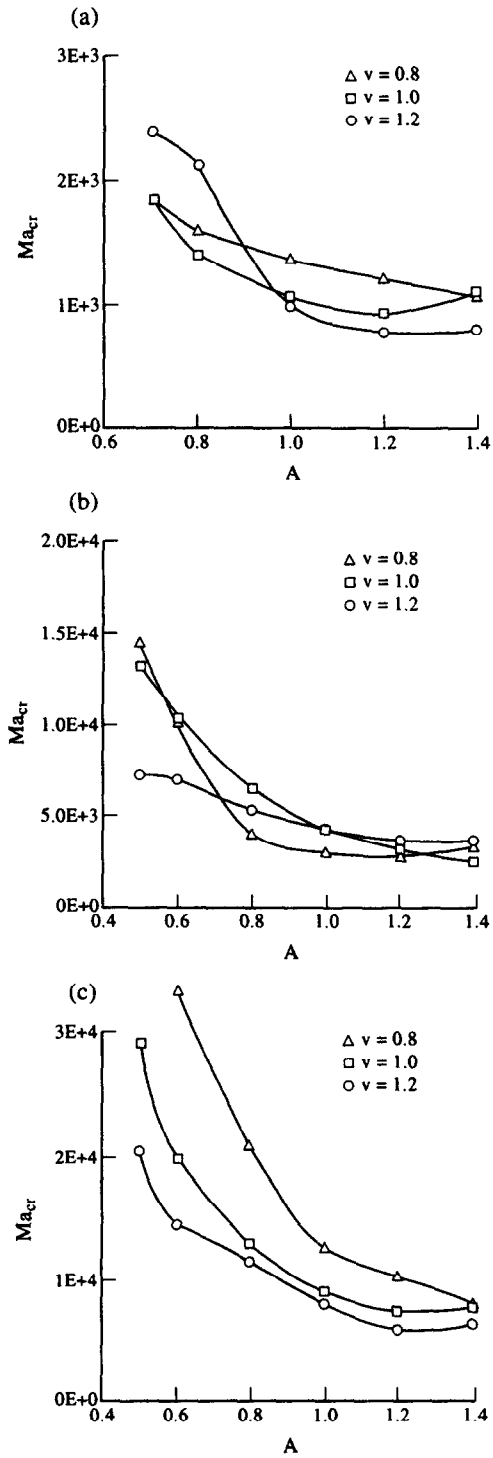

Fig. 9. The critical Marangoni number for the most unstable mode $m = 1$ vs aspect ratio of liquid bridge for $V = 0.8$, 1.0 and 1.2 and (a) $Pr = 1$, (b) $Pr = 10$, and (c) $Pr = 50$.

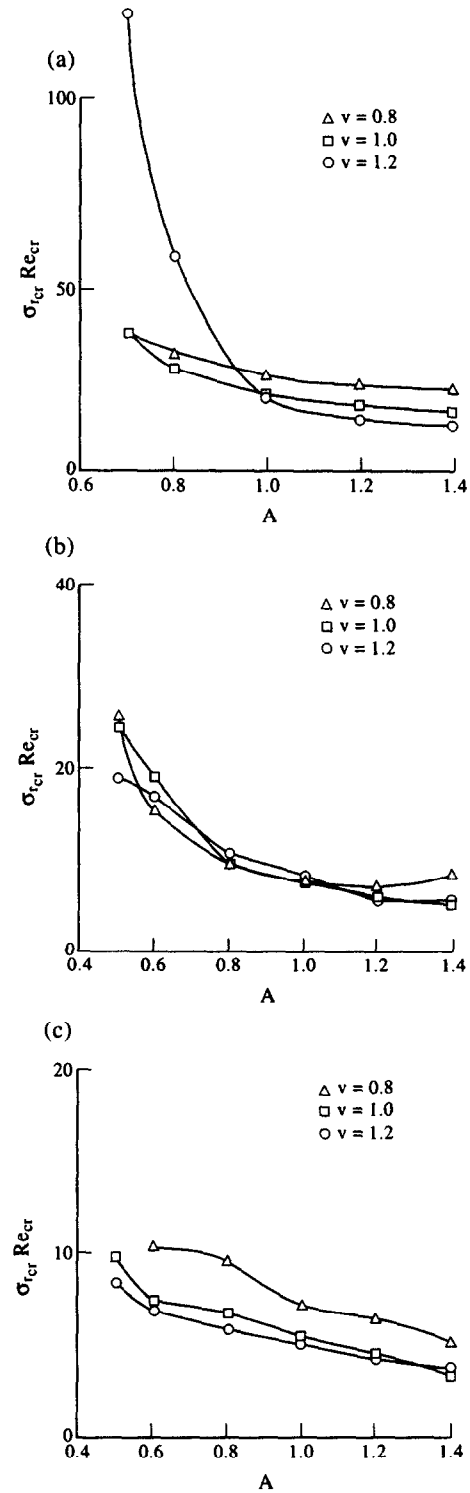

Fig. 10. The critical frequency for the most unstable mode $m = 1$ vs aspect ratio of liquid bridge for $V = 0.8$, 1.0 and 1.2 and (a) $Pr = 1$, (b) $Pr = 10$, and (c) $Pr = 50$.

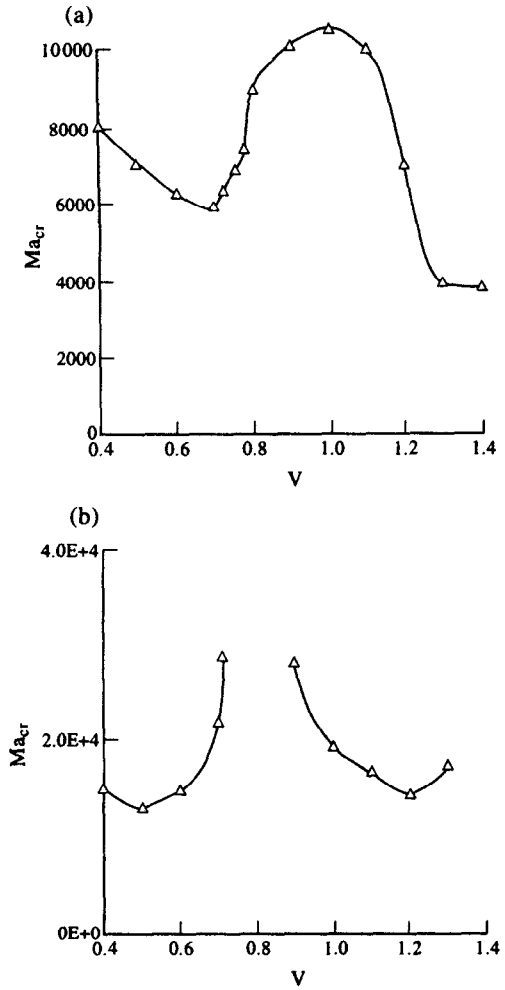

Fig. 11. The critical Marangoni number for the most unstable mode $m = 1$ vs the liquid bridge volume for $A = 0.6$ and (a) $Pr = 10$, (b) $Pr = 50$.

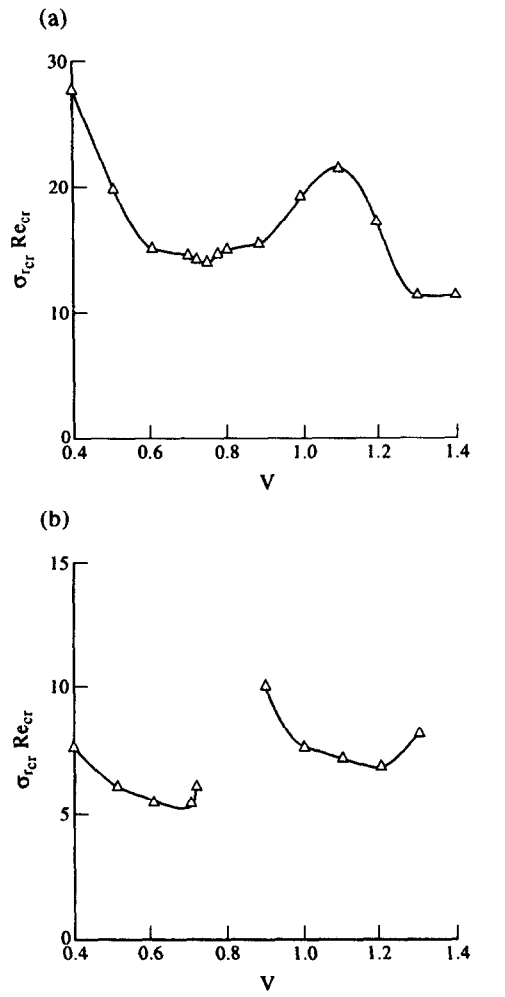

Fig. 12. The critical frequency for the most unstable mode $m = 1$ vs the liquid bridge volume for $A = 0.6$ and (a) $Pr = 10$, (b) $Pr = 50$.

Marangoni number versus volume size are obtained. Critical frequencies are non-uniformly distributed with the volume size.

The critical curves of the Marangoni number are strongly influenced by the liquid bridge volume. The features of the critical curves of Marangoni number are also influenced by the Prandtl number, the instability feature of thermocapillary convection for the case of small Prandtl number $Pr < 1$ will be discussed in the future.

REFERENCES

1. Pearson, J. R. A., *Journal of Fluid Mechanics*, 1958, **4**, 489.
2. Smith, M. K. and Davis, S. H., *Journal of Fluid Mechanics*, 1983, **132**, 119.
3. Xu, J. J. and Davis, S. H., *Physics of Fluids*, 1984, **27**, 1102.
4. Kuhlmann, H., *Microgravity Science and Technology*, 1994, **7**, 75.
5. Kuhlmann, H., *Physics of Fluids A*, 1989, **1**, 672.
6. Hu, W. R. and Tang, Z. M., *Science China A*, 1990, **33**, 934.
7. Hu, W. R., Shu, J. Z., Zhou, R. and Tang, Z. M., *Journal of Crystal Growth*, 1994, **142**, 379.
8. Tang, Z. M. and Hu, W. R., *Journal of Crystal Growth*, 1994, **142**, 385.
9. Chen, Q. S. and Hu, W. R., *International Journal of Heat and Mass Transfer*, 1997, **40**, 757.
10. Velten, R., Schwabe, D. and Scharmann, A., *Physics of Fluids A*, 1991, **3**, 267.